Electronic Supplementary Information

Phase and composition controlled synthesis of cobalt sulfides hollow nanospheres for electrocatalytic water splitting

Xiaoya Ma, Wei Zhang, Yida Deng, Cheng Zhong, Wenbin Hu and Xiaopeng Han*

Tianjin Key Laboratory of Composite and Functional Materials, Key Laboratory of Advanced Ceramics and Machining Technology (Ministry of Education), School of Materials Science and Engineering, Tianjin University, Tianjin 300072, China.

*E-mail: xphan@tju.edu.cn

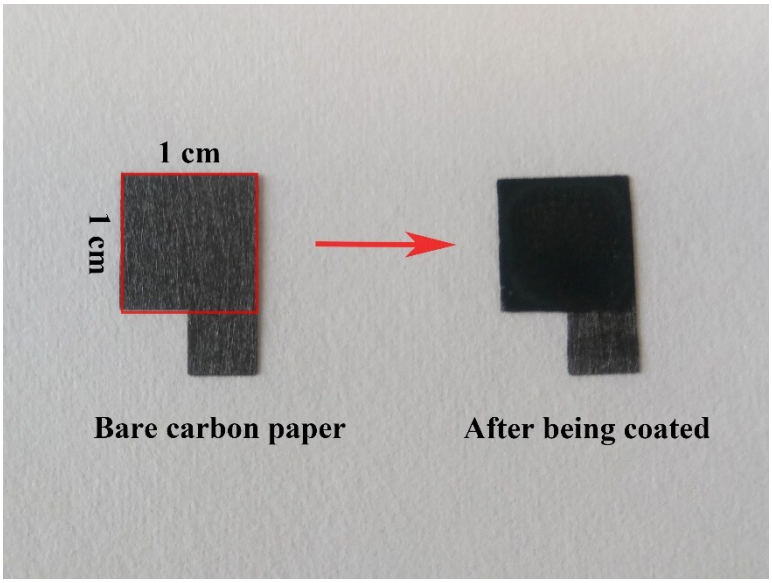

Fig. S1 Digital images of carbon papers before and after coating the active material slurry**.**

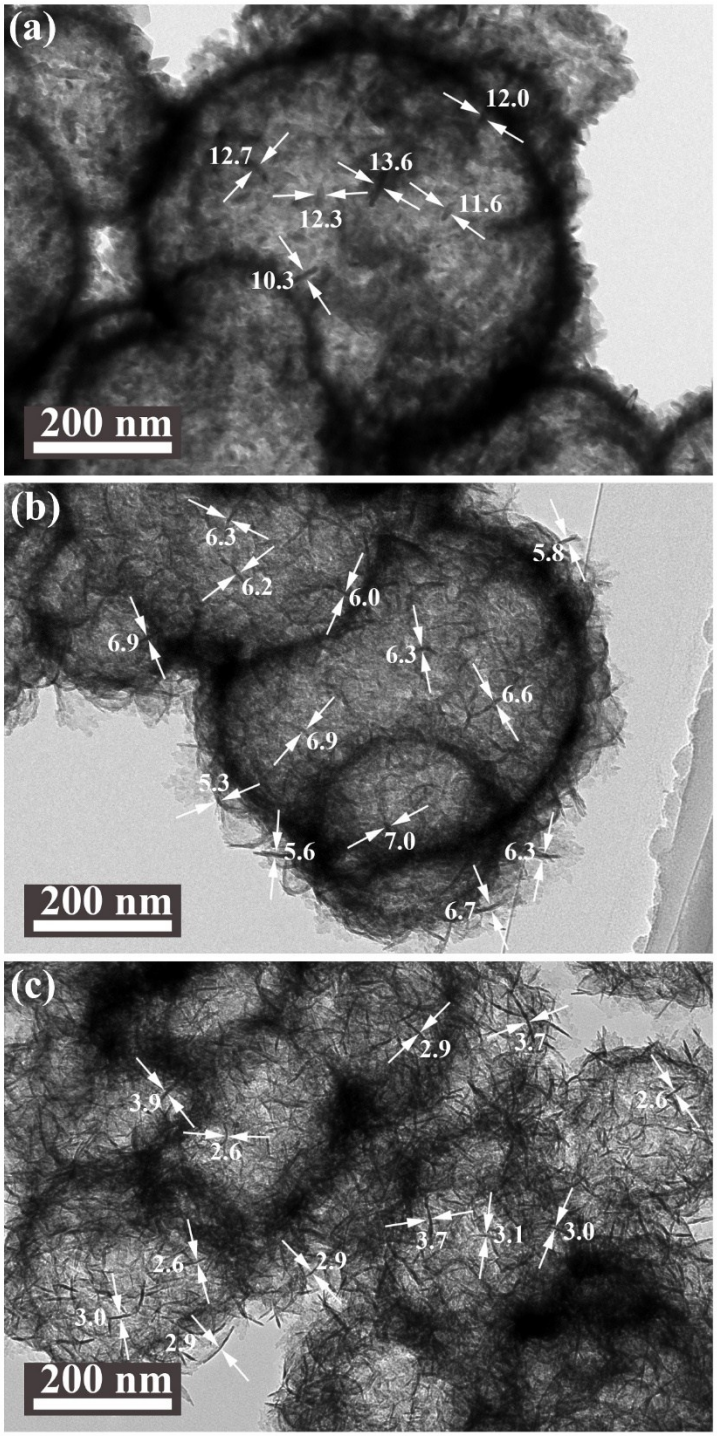

Fig. S2 TEM images of (a) Co_9S_8, (b) Co_3S_4 and (c) CoS_2 HNSs. The results show that as the molar ratio of sulfur to cobalt source increases, the sphere structure becomes looser and the surface of nanosheets become thinner.

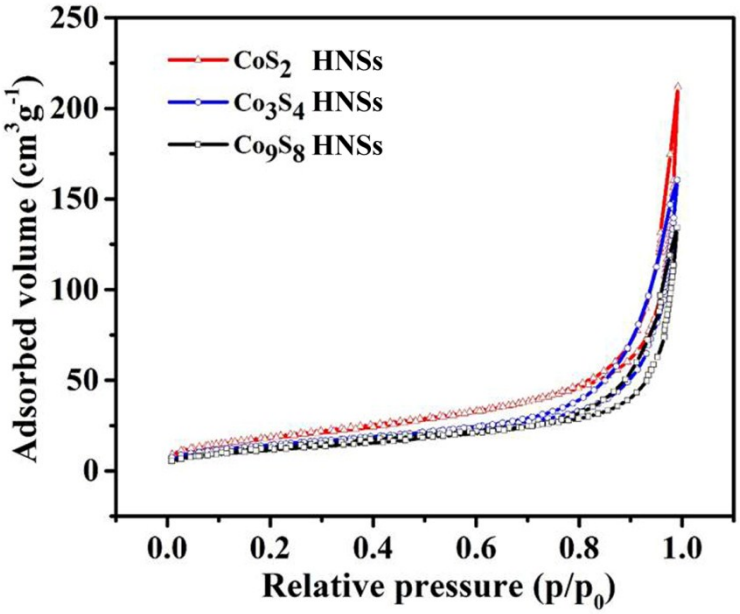

Fig. S3 N_2 adsorption–desorption isotherms of Co_9S_8, Co_3S_4 and CoS_2 HNSs.

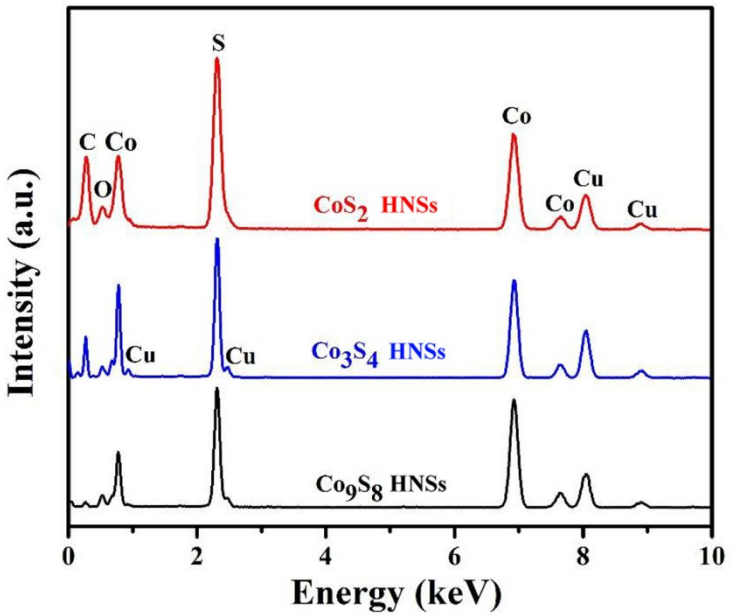

Fig. S4 EDS spectra of Co_9S_8, Co_3S_4 and CoS_2 HNSs.

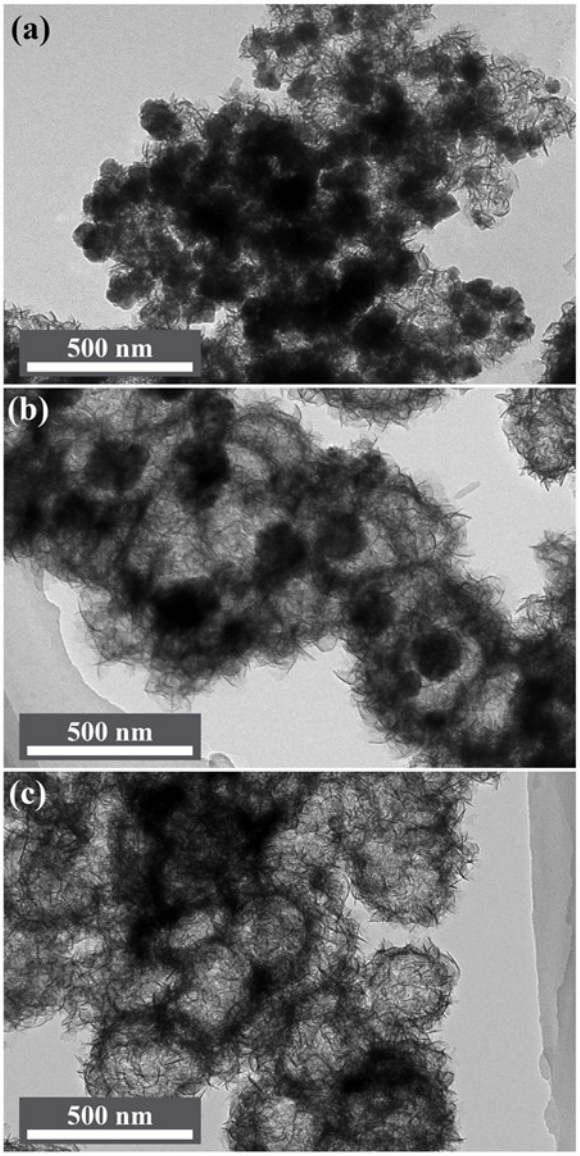

Fig. S5 TEM images of CoS_2 samples obtained at different reaction time: (a) 3 h, (b) 6 h, (c) 9 h.

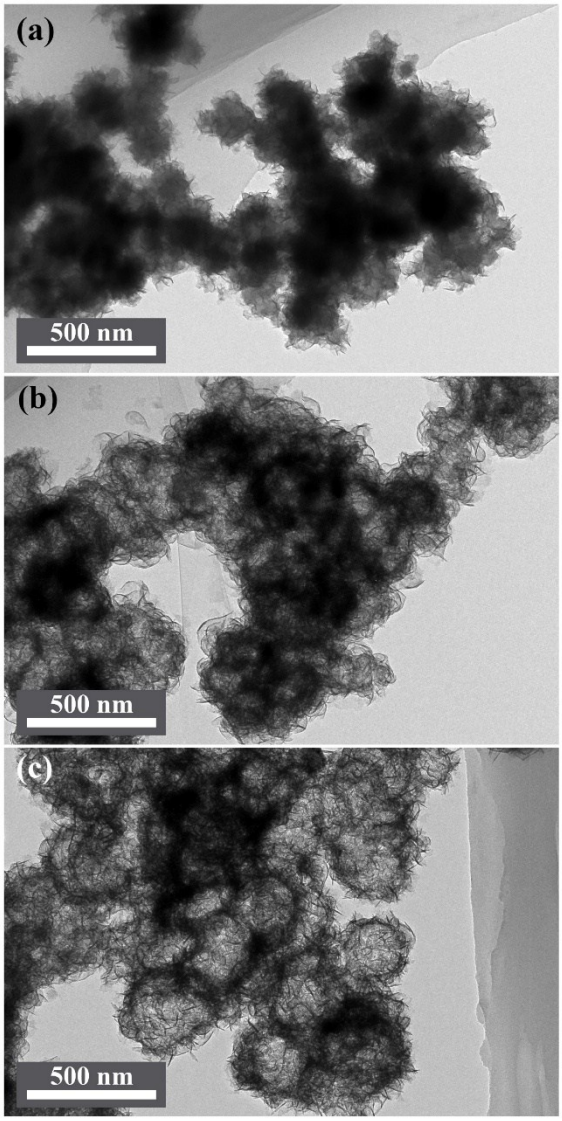

Fig. S6 TEM images of CoS_2 samples obtained at different reaction temperature: (a) 120 °C, (b) 160 °C, (c) 200 °C.

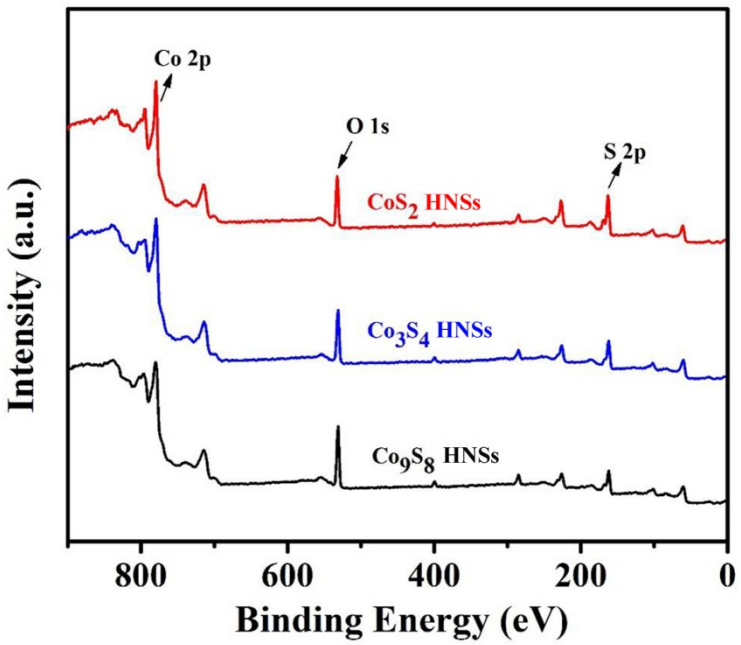

Fig. S7 XPS survey spectra of Co_9S_8, Co_3S_4 and CoS_2 HNSs.

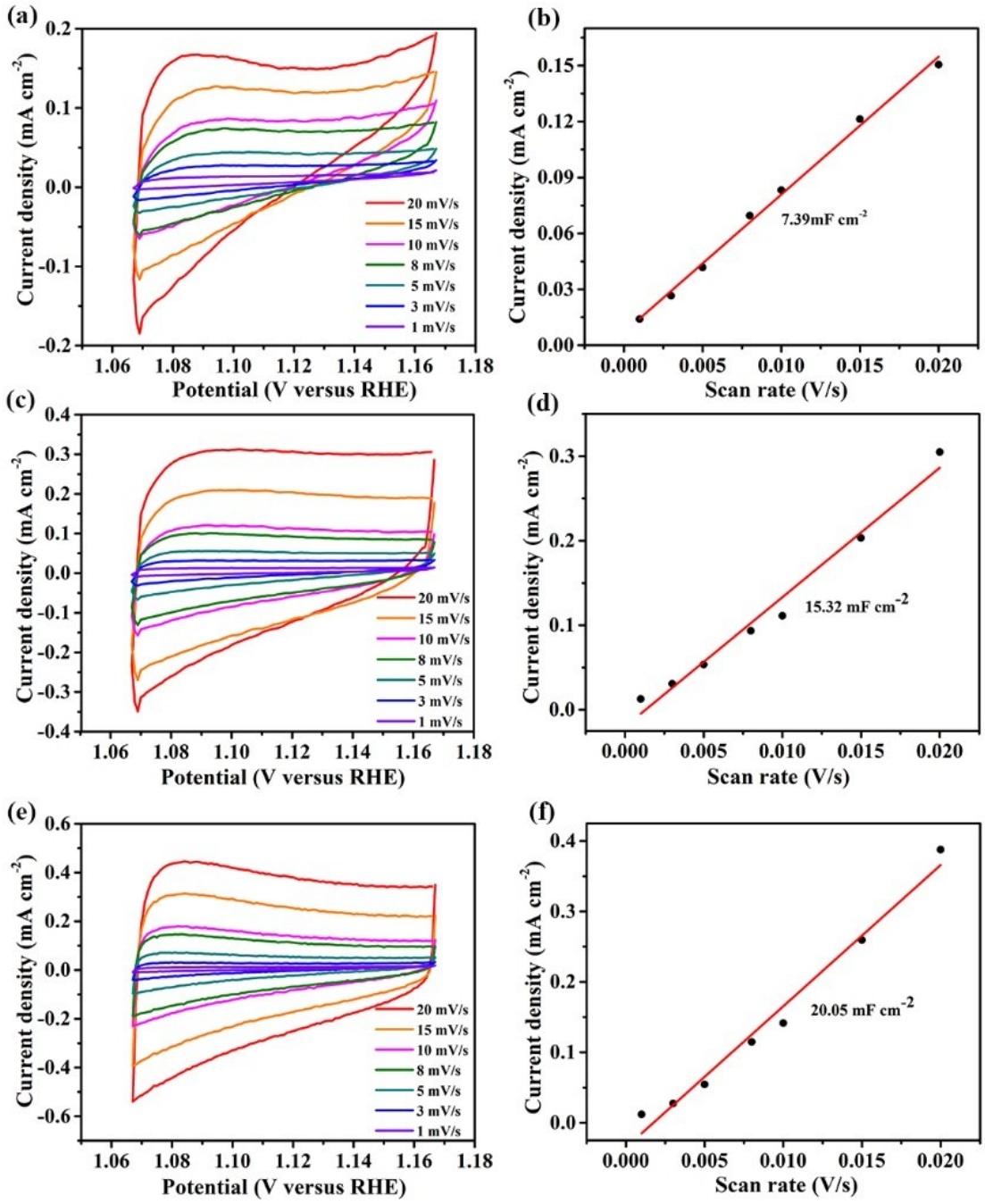

Fig. S8 Cycle voltammograms from 1.067 to 1.167 V vs RHE in 1.0 M KOH at different scan rates and the corresponding linear fitting of the capacitive density versus scan rates of (a, b) Co_9S_8, (c, d) Co_3S_4, and (e, f) CoS_2 HNSs.

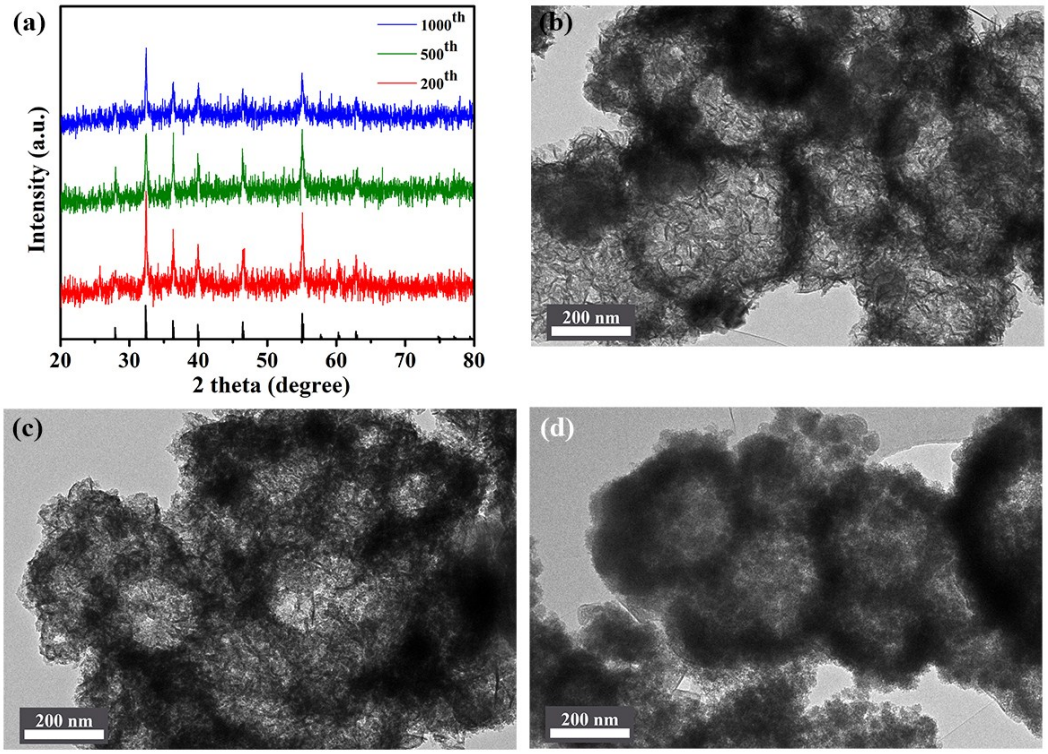

Fig. S9 (a) XRD patterns and (b-d) TEM image of CoS_2 HNSs after 200 (b), 500 (c), and 1000 (d) OER cycles.

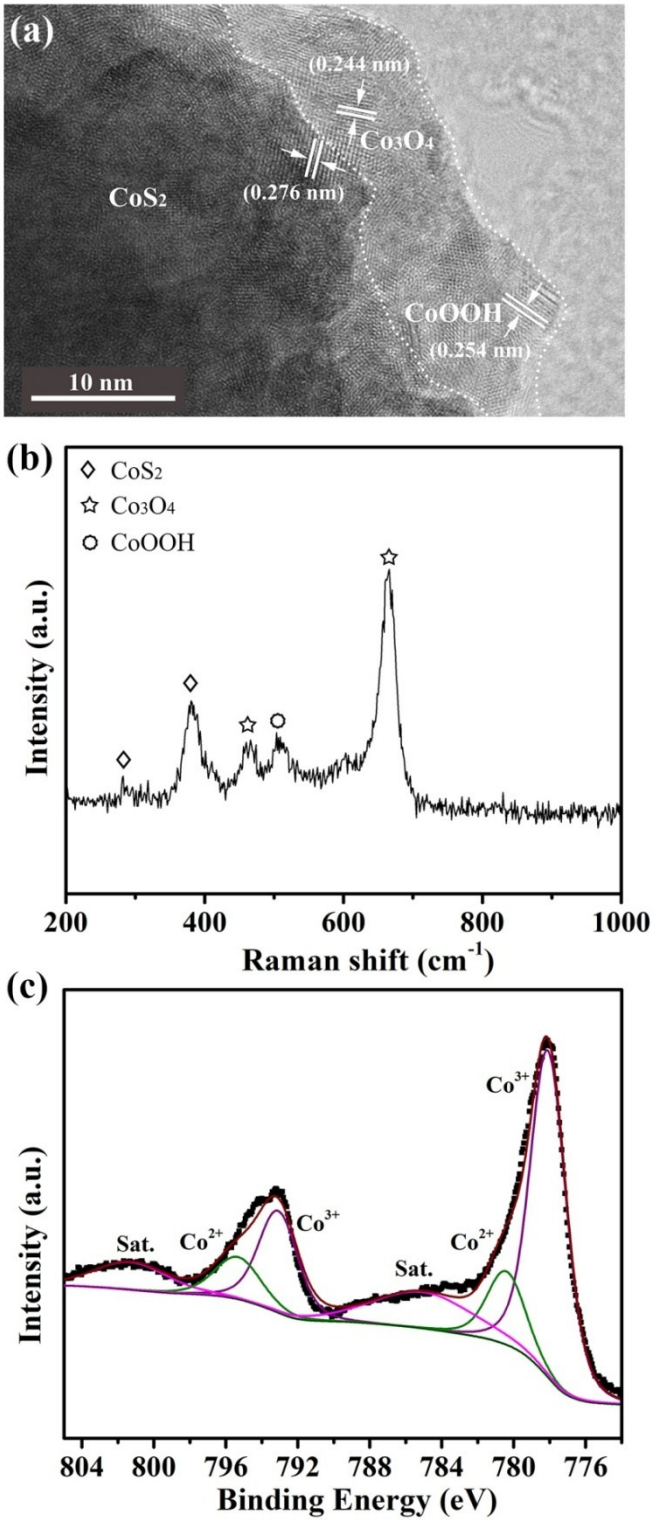

Fig. S10 (a) HRTEM, (b) Raman and (c) Co 2p XPS spectrum of CoS_2 HNSs after 1000 OER cycles. HRTEM and Raman results reveal the formation of Co_3O_4/CoOOH after 1000 OER cycles. In XPS spectrum, the ratio of Co^{3+} to Co^{2+} is much higher than original CoS_2 (Fig. 4a), which confirms the formation of higher valence state of Co after OER cycles.

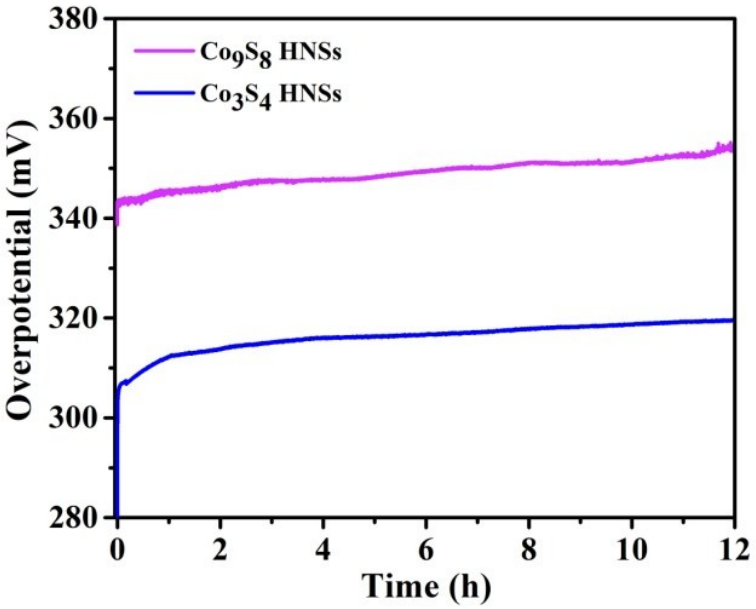

Fig. S11 Chronopotentiometric response of Co_3S_4 and Co_9S_8 HNSs at a constant OER current density of 10 mA cm^{-2}.

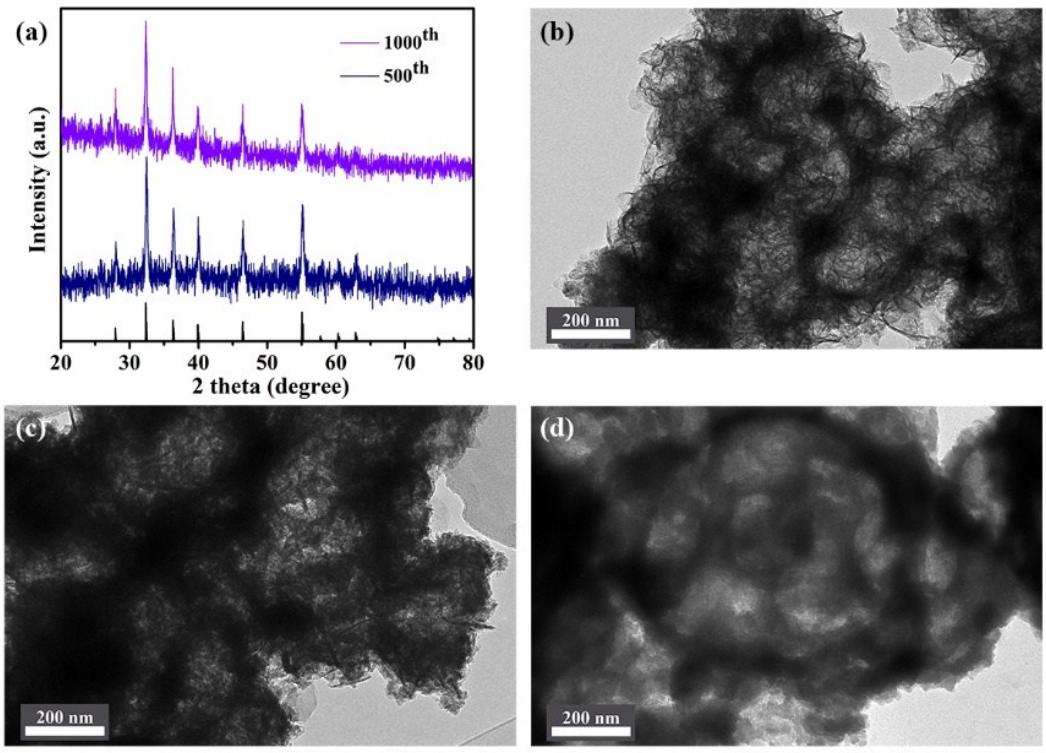

Fig. S12 (a) XRD patterns and (b-d) TEM image of CoS_2 HNSs after 200 (b), 500 (c), and 1000 (d) HER cycles.

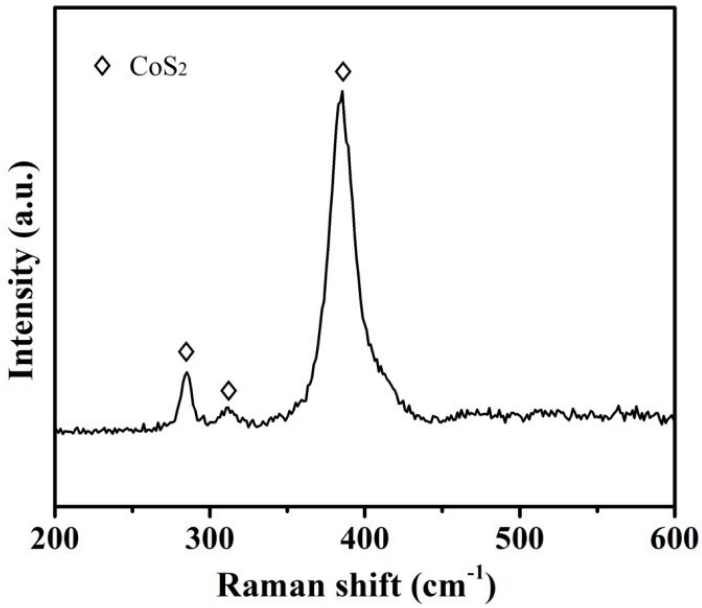

Fig. S13 Raman spectrum of CoS_2 HNSs after 1000 HER cycles.

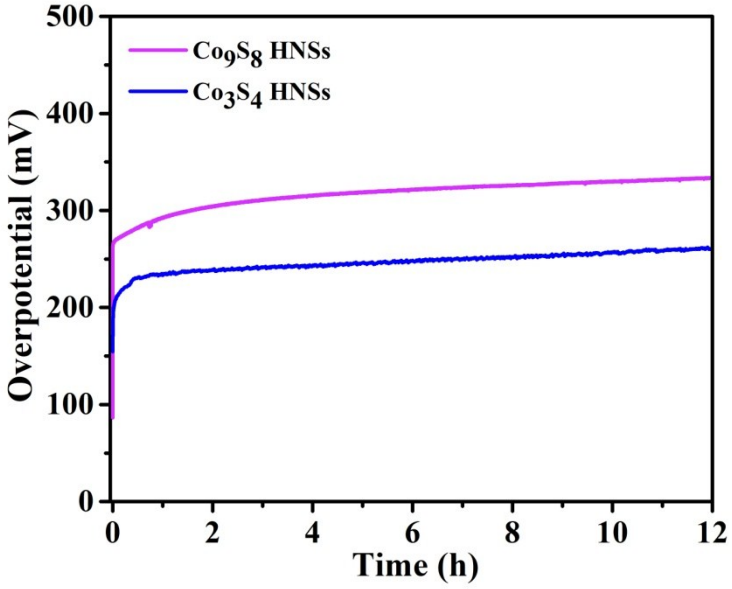

Fig. S14 Chronopotentiometric response of Co_3S_4 and Co_9S_8 HNSs at a constant HER current density of 10 mA cm^{-2}.

Table S1. Co and S atomic percentage in Co_9S_8, Co_3S_4, and CoS_2 HNSs from EDS spectra.

Catalysts	Percentage of Co (%)	Percentage of S (%)
CoS_2 HNSs	32.60	67.40
Co_3S_4 HNSs	42.75	57.25
Co_9S_8 HNSs	48.58	51.42

Table S2. Comparison of OER performances of CoS_2 HNSs with other reported similar non-noble metal OER electrocatalysts.

Catalyst	Electrode	Electrolyte	Loading density (mg cm^{-2})	Current density (mA cm^{-2})	Overpotential （mV）	Refs
Co_9S_8 hollow microplates	glassy carbon electrode	1.0M KOH	0.37	10	278	1
FeB_2	glassy carbon electrode	1.0M KOH	0.2	10	296	2
Co-P film	copper foil	1.0M KOH	2.71	10	345	3
Ni_3S_2/Ni	Ni foam	0.1M KOH	37.00	10	187	4
$Ni_xCo_{3-x}O_4$ nanowire	Ti foil	1.0M KOH	3.00	10	370	5
NiFe-LDH/rGO	Ni foam	1.0M KOH	0.5	10	250	6
$NiCo_2S_4$@N/S-rGO	glassy carbon electrode	0.1 M KOH	0.283	10	470	7
NiCo hydroxide nanosheets	MOFs	1.0M KOH	0.17	10	324	8
Mn-Co oxyphosphide	glassy carbon electrode	1.0 M KOH	0.25	10	370	9
NiP nanoparticle film	copper foam	1.0 M KOH	5	10	325	10
CoS_2 HNSs	Carbon paper	1.0M KOH	1.5	10 20	290 305	This work

Table S3. Comparison of the HER Performances of CoS_2 HNSs with other reported similar non-noble metal HER electrocatalysts.

Catalyst	Electrode	Electrolyte	Loading density (mg cm^{-2})	Current density (mA cm^{-2})	Overpotential (mV)	Refs
CoOx@CN	glassy carbon electrode	1.0M KOH	0.54	10	232	11
Ni/MWCNT	stainless steel meshes	1.0M KOH	----	10	350	12
Co–Ni–B@NF	Ni foam	1.0M KOH	----	10	205	13
Ni/Mo_2C-PC	glassy carbon electrode	1.0M KOH	0.5	10	179	14
Co-NRCNTs	glassy carbon electrode	1.0M KOH	0.28	10	370	15
Zn-Co-S nanoneedles	Carbon fiber paper	1.0M KOH	0.6	10	234	16
MoB	carbon paste electrode	1.0M KOH	2.30	10	210	17
MoS_2-WS_2	Ni foam	1.0M KOH	----	10	275	18
FeP NAs	Carbon cloth	1.0M KOH	1.5	20	370	19
CoS_2 HNSs	Carbon paper	1.0 M KOH	1.5	10 20	193 223	This work

Table S4. Comparison of two-electrode water-splitting voltage of CoS_2 HNSs/CP catalyst with other reported bifunctional electrocatalysts.

Catalyst	Electrolyte	Current density (mA cm^{-2})	Overall voltage (V)	References
$NiCo_2S_4$@NiFe LDH/NF	1.0M KOH	10	1.6	20
CoFe LDH-F	1.0M KOH	10	1.63	21
EG/$Co_{0.85}$Se/NiFe-LDH	1.0M KOH	10	1.67	22
NiFe/$NiCo_2S_4$/NF	1.0M KOH	10	1.67	23
CoP_x/NC	1.0M KOH	10	1.71	24
Ni/Mo_2C-PC	1.0M KOH	10	1.66	14
Zn-Co-S NN/CFP	1.0M KOH	10	1.72	16
Ni_5P_4/NF	1.0M KOH	10	1.69	25
Ni_3S_2/NF	1.0M KOH	13	1.76	26
CoS_2 HNSs/CP	1.0 M KOH	10	1.68	This work

References

S1. H. Liu, F. X. Ma, C. Y. Xu, L. Yang, Y. Du, P. P. Wang, S. Yang and L. Zhen, *ACS Appl. Mater. Interfaces*, 2017, **9**, 11634-11641.

S2. H. Li, P. Wen, Q. Li, C. Dun, J. Xing, C. Lu, S. Adhikari, L. Jiang, D. L. Carroll and S. M. Geyer, *Adv. Energy Mater.*, 2017, **7**, 1700513.

S3. N. Jiang, B. You, M. Sheng and Y. Sun, *Angew. Chem. Int. Ed.*, 2015, **54**, 6251-6254.

S4. W. Zhou, X. J. Wu, X. Cao, X. Huang, C. Tan, J. Tian, H. Liu, J. Wang and H. Zhang, *Energy Environ. Sci.*, 2013, **6**, 2921-2924.

S5. Y. Li, P. Hasin and Y. Wu, *Adv. Mater.*, 2010, **22**, 1926-1929.

S6. T. Zhan, Y. Zhang, X. Liu, S. Lu and W. Hou, *J. Power Sources*, 2016, **333**, 53-60.

S7. Q. Liu, J. Jin and J. Zhang, *ACS Appl. Mater. Interfaces*, 2013, **5**, 5002-5008.

S8. H. Liang, F. Meng, M. Caban-Acevedo, L. Li, A. Forticaux, L. Xiu, Z. Wang and S. Jin, *Nano Lett.*, 2015, **15**, 1421-1427.

S9. B. Y. Guan, L. Yu and X. W. Lou, *Angew. Chem. Int. Ed.*, 2017, **56**, 2386-2389.

S10. Q. Liu, S. Gu and C. M. Li, *J. Power Sources*, 2015, **299**, 342-346.

S11. H. Y. Jin, J. Wang, D. F. Su, Z. Z. Wei, Z. F. Pang and Y. Wang, *J. Am. Chem. Soc.*, 2015, **137**, 2688-2694.

S12. M. A. McArthur, L. Jorge, S. Coulombe and S. Omanovic, *J. Power Sources*, 2014, **266**, 365-373.

S13. N. Xu, G. Cao, Z. Chen, Q. Kang, H. Dai and P. Wang, *J. Mater. Chem. A*, 2017, **5**, 12379-12384.

S14. Z. Y. Yu, Y. Duan, M. R. Gao, C. C. Lang, Y. R. Zheng and S. H. Yu, *Chem. Sci.*, 2017, **8**, 968-973.

S15. X. Zou, X. Huang, A. Goswami, R. Silva, B. R. Sathe, E. Mikmekova and T. Asefa, *Angew. Chem. Int. Ed.*, 2014, **53**, 4372-4376.

S16. X. Wu, X. Han, X. Ma, W. Zhang, Y. Deng, C. Zhong and W. Hu, *ACS Appl. Mater. Interfaces*, 2017, **9**, 12574-12583.

S17. H. Vrubel and X. Hu, *Angew. Chem. Int. Ed.*, 2012, **51**, 12703-12706.

S18. S. K. Kim, W. Song, S. Ji, Y. R. Lim, Y. B. Lee, S. Myung, J. Lim, K.-S. An and S. S. Lee, *Appl. Surf. Sci.*, 2017, **425**, 241-245.

S19. Y. Liang, Q. Liu, A. M. Asiri, X. Sun and Y. Luo, *ACS Catal.*, 2014, **4**, 4065-4069.

S20. J. Liu, J. Wang, B. Zhang, Y. Ruan, L. Lv, X. Ji, K. Xu, L. Miao and J. Jiang, *ACS Appl. Mater. Interfaces*, 2017, **9**, 15364-15372.

S21. P. F. Liu, S. Yang, B. Zhang and H. G. Yang, *ACS Appl. Mater. Interfaces*, 2016, **8**, 34474-34481.

S22. Y. Hou, M. R. Lohe, J. Zhang, S. Liu, X. Zhuang and X. Feng, *Energy Environ. Sci.*, 2016, **9**, 478-483.

S23. C. Xiao, Y. Li, X. Lu and C. Zhao, *Adv. Funct. Mater.*, 2016, **26**, 3515-3523.

S24. B. You, N. Jiang, M. Sheng, S. Gul, J. Yano and Y. Sun, *Chem. Mater.*, 2015, **27**, 7636-7642.

S25. M. Ledendecker, S. Krick Calderon, C. Papp, H. P. Steinruck, M. Antonietti and M. Shalom, *Angew. Chem. Int. Ed.*, 2015, **54**, 12361-12365.

S26. L. L. Feng, G. Yu, Y. Wu, G. D. Li, H. Li, Y. Sun, T. Asefa, W. Chen and X. Zou, *J. Am. Chem. Soc.*, 2015, **137**, 14023-14026.